Synthesis, physico-chemical characterisation and bacteriostatic study of Pt-complexes with substituted amine ligands

B. Barta Holló[1], I. M. Szilágyi[2,3], Cs. jr. Várhelyi[4], D. Hunyadi[2], R.I. Nagy[4], N.G. Tihi[4], F. Goga[4], J. Papp[5], R. Szalay[6], G. Pokol[2]

[1]*Faculty of Sciences, University of Novi Sad, 21000–Novi Sad, Trg Dositeja Obradovića 3, Serbia*
[2]*Department of Inorganic and Analytical Chemistry, Budapest University of Technology and Economics, H–1111 Budapest, Szt. Gellért tér 4, Hungary*
[3]*MTA-BME Technical Analytical Chemistry Research Group, H–1111 Budapest, Szt. Gellért tér 4, Hungary*
[4]*Faculty of Chemistry, Babeş-Bolyai University, 400 028–Cluj-Napoca, Arany J. str. 11, Romania*
[5]*Faculty of Biology and Geology, Babeş-Bolyai University, 400 084–Cluj-Napoca, M. Kogălniceanu str. 1, Romania*
[6]*Institute of Chemistry, Eötvös Loránd University, H–1117 Budapest, Pázmány P. sétány 1/a, Hungary*

Abstract

Three complexes of general formula $PtCl_2R_2$ were synthesized, where R is the amine ligand with aromatic substituents. Coordination compounds [Pt(*an*)$_2$Cl$_2$] (**1**), [Pt(*pa*)$_2$Cl$_2$] (**2**) and [Pt(*aph*)$_2$Cl$_2$] (**3**), where *an* is 2-aminonaphtalene, *pa* is 2-pyrimidinamine and *aph* is 4-anilinophenol, were characterized by on-line coupled TG/DTA-MS, powder XRD and spectroscopic techniques (FTIR, ESI-MS and NMR), and tested against selected Gram(+) and Gram(–) bacteria. The thermal data show that all three compounds contain lattice or absorbed water, and the stability of the anhydrous compounds in nitrogen decreases in the order **2** > **1** > **3**. Above 200 °C, the complexes loose characteristic fragments of their ligands. The spectroscopic data are in accordance with the thermal properties of the samples and prove their composition. The compounds are more effective inhibitors of Gram(+) than Gram(−) bacteria.

Keywords

Pt(II)-complexes, amine ligand, thermal properties, spectroscopic data, antimicrobial activity

Corresponding author

B. Barta Holló,
Department of Chemistry, Biochemistry and Environmental Protection, Faculty of Sciences, University of Novi Sad,
21000 Novi Sad, Trg Dositeja Obradovića 3, Serbia,
E-mail address: hberta@uns. ac.rs

Introduction

Metallodrugs based on platinum coordination complexes are very important class of drugs [1]. Since the discovery of anticancer activity of cisplatin, high efforts have been made to find more active and less toxic neoplastic agents for cancer treatment in humans [2]. High number of different platinum complexes is synthesized with the aim to understand better the mode of action of platinum based antitumor drugs and to get new ones with fewer side effects. [3,4,5] Cisplatin and its analogues bind to the DNA in cancer cells [6,7,8]. These binding properties are studied and used in design and synthesis of new antibacterial drugs also [9,10]. As a high number of pathogenic bacteria show resistance toward antibiotics, it is necessary to find new effective compounds and control the multidrug resistance of microbes [11,12]. Therefore much effort is put into modifying of antibiotics already in use, while new compounds are also synthesized. Some tetracyclines, coordinated to Pt(II), showed improved antimicrobial activity [13]. To obtain new Pt(II) metallodrugs, usually N donor ligands are used, beside the Schiff-bases [14,15], often substituted or aromatic amines [16,17,18,19]. Due to their relatively simple synthetic procedures and structures, they are good candidates as anticancer or antimicrobial agents.

Thermal properties of potentially biological active compounds are essential to their future usage. Therefore thermal analysis is a common part of characterizing compounds with biological activity [20,21,22,23,24,25]. Thermoanalytical methods provide important information on the thermal stability, polymorphic forms or structural changes [26,27,28], and purity of potential new drugs [29,30,31,32].

In continuation of our earlier work on synthesis, physical and chemical characterization of iron(II) complexes with amine ligands [33] in this paper Pt(II) coordination compounds with different amine ligands are described. The aim of this study was the synthesis, physical, chemical and antimicrobial characterization of biologically active compounds of general formula $PtCl_2R_2$ under the same reaction conditions, where R is a selected amine ligand. Since the thermal properties of biological active compounds are crucial for their future application, the other aim of this work is the detailed thermal analysis of the synthesized coordination compounds. Namely, [Pt(*an*)$_2$Cl$_2$] (**1**), [Pt(*pa*)$_2$Cl$_2$] (**2**) and [Pt(*aph*)$_2$Cl$_2$] (**3**) were prepared, where *an* is 2-aminonaphthalene, *pa* is 2-pyrimidinamine and *aph* is 4-anilinophenol. Different synthetic methods and properties of compounds **1** [34] and **2** [35] were published earlier. Here we describe alternative synthetic routes for **1** and **2**, and also the synthesis of a new complex of Pt (**3**). The detailed physicochemical characterization of the complexes by TG/DTA-MS, XRD, FTIR, NMR, ESI-MS, and antimicrobial tests are presented and discussed in the view of thermal properties.

Experimental data

Synthesis of the complexes:

In all synthetic procedures platinum(II) chloride ($PtCl_2$) was used as reactant, which was previously prepared by reduction of platinum(IV) chloride ($PtCl_4$); e.g. 1.25 mmol (0.42 g) $PtCl_4$ was reduced with 1 cm^3 formic acid in 10 cm^3 distilled water at room temperature. The complexes were synthesized starting from the as-obtained $PtCl_2$ solution, which was reacted with 2.5 mmol of substituted amines (2-aminonaphtalene for **1**, 2-pyrimidinamine for **2** and 4-anilinophenol for **3**) in 10 cm^3 methanol. The reaction mixtures were boiled for 3 hours on water-bath. Following the color change of the mixtures, the coordination compounds began to precipitate. After leaving the reaction mixtures at room temperature to complete the precipitation (24 h), the compounds were filtered and washed with methanol.

Yields, molar masses and FTIR data of the obtained complexes:

1·2H$_2$O; [Pt(*an*)$_2$Cl$_2$]·2H$_2$O: Yield: 35.6 %. Mr = 588.39; IR [cm^{-1}]: 3188, 1599, 1485, 1448, 1349, 1146, 999, 951, 853, 779, 744, 685, 494, 441, 414.
2; [Pt(*pa*)$_2$Cl$_2$]: Yield: 29.2 %. Mr = 456.20; IR [cm^{-1}]: 3294, 3082, 1618, 1586, 1476, 1351, 1132, 1088, 986, 871, 784, 768, 671, 494, 445, 413.
3; [Pt(*aph*)$_2$Cl$_2$]: Yield: 41.0 %. Mr = 636.43; IR [cm^{-1}]: 3732, 3647, 3232, 3056, 1643, 1595, 1489, 1367, 1162, 1103, 1001, 865, 752, 692, 619, 496, 452, 415.

Methods
TG/DTA-MS data were collected using a TA Instruments SDT 2960 DTA/TG device coupled on-line through a heated (T = 200 °C) 100 % methyl deactivated fused silica capillary tube of 0.15 mm inner diameter with a Balzers Instruments ThermoStar GSD 300T quadrupole mass spectrometer. The measurements were carried out at 10 °C min^{-1} heating rate in N_2 and air atmospheres (flow rate: 130 cm^3 min^{-1}) in an open platinum crucible and with sample sizes of 1–3 mg. Selected ions between m/z = 1–190 were monitored through 64 channels in Multiple Ion Detection Mode (MID) with a measuring time of 0.5 s per channel.
IR data were collected on a Bruker Alpha FTIR spectrometer (platinum single reflection diamond ATR) at room temperature in the middle infrared range of 4000–400 cm^{-1}.
Mass spectra of the samples, dissolved in MeOH, were collected with a PE Sciex API 2000 triple quadrupole mass spectrometer using electrospray ionization (ESI).
NMR spectra were recorded in DMSO-d_6 solution in 5 mm tubes at R.T. on a Bruker DRX 500 spectrometer at 500 MHz using TMS as internal reference.
Powder X-ray diffraction (XRD) measurements were carried out on a PANalytical X'pert Pro MPD X-ray diffractometer equipped with an X'Celerator type detector. The samples were measured at room temperature in powder form.

Antimicrobial activity
The coordination compounds for antimicrobial *in vitro* activity were tested against Gram(+) bacteria *Staphylococcus aureus*, *Bacillus subtilis*, *Sarcina ventriculi* and Gram(−) bacteria *Klebsiella oxytoca* and *Escherichia coli*. For the antimicrobial sensitivity test the Kirby-Bauer disk diffusion method was applied [36,37].
100 μL of the tested bacterial cultures were spread on nutrient agar medium and after inoculation filter paper discs (5 mm in diameter) containing 10 μL sample solutions were placed on the surface of the solid medium. The Petri plates were incubated at 37 °C for 18 – 24 h. After incubation the diameters of inhibition zones were measured.

Results and discussion

All compounds were synthesized in the same way. Platinum(IV) chloride was reduced by formic acid then reacted with the selected amine ligands. The original procedure for the synthesis of the complexes with 2-aminonaphtalene (**1**) and 2-pyrimidinamine (**2**) [34, 35] was partially modified. In contrast to methods reported earlier, where E. Gabano et al. [34] used $K_2[PtCl_4]$ for the synthesis of **1** and L.K. Mishra [35] reacted $PtCl_2$ with 2-pyrimidinamine in a molar ratio of 1:2.5, respectively, the metal−to−ligand molar ratio was adjusted to 1:2 in our cases. Besides, a new coordination compound with 4-anilinophenol (*aph*) ligand was also synthesized (**3**). The structures of complexes are shown on Scheme 1. In all compounds two chloride ions and two monodentate amine ligands are coordinated to Pt(II). Ligands *an* and *pa* in **1** and **2** are primary amines with bicyclic (**1**) and heterocyclic (**2**) aromatic substituent. Differently, complex **3** is prepared using a secondary amine, 4-anilinophenol substituted with benzene and phenol rings.

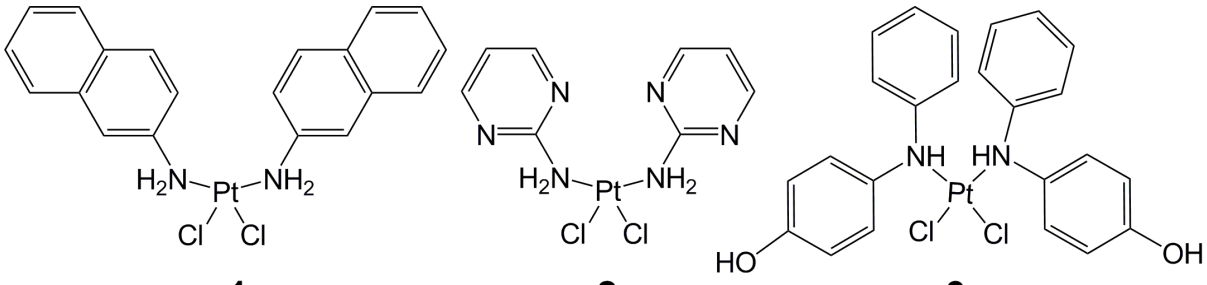

1 **2** **3**

Scheme 1 The structure of [Pt(*an*)$_2$Cl$_2$] (**1**), [Pt(*pa*)$_2$Cl$_2$] (**2**) and [Pt(*aph*)$_2$Cl$_2$] (**3**)

The powder-XRD measurements show that the samples precipitated in amorphous form; hence, their structure is characterized further by spectroscopic methods and elemental analysis.

Elemental analysis

The elemental analysis data (table 1) of the compounds **1**-**3** prove the proposed compositions (scheme 1.) and show the solvent content of the samples. Complex **1** crystallizes with two water molecules, while **2** and **3** do not contain crystal water.

Table 1 Elemental analysis data of the complexes **1**-**3**

	C / %		H / %		N / %	
Compound	Anal.	Calc.	Anal.	Calc.	Anal.	Calc.
1·2H$_2$O; $PtC_{20}H_{22}Cl_2N_2O_2$	40.91	40.83	3.12	3.77	4.44	4.76
2; $PtC_8H_{10}Cl_2N_6$	17.16	17.06	2.22	2.18	14.53	14.48
3; $PtC_{24}H_{22}N_2O_2Cl_2$	45.80	45.29	3.64	3.48	4.92	4.40

Mass spectrometric measurements

In the mass spectra of all complexes, the molecular ions were successfully detected. Table 2 presents the characteristic fragments for each complex.

Table 2 Mass spectral data of the complexes

Formula	Molecular mass	m/z [fragments]
[Pt(*an*)$_2$Cl$_2$]·2H$_2$O [Pt(*an*)$_2$Cl$_2$] (**1**)	588.4 552.4	586.8 [M·2OH]$^+$, 552.8 [M]$^+$, 480 [Pt(*an*)$_2$]$^+$, 425 [-HN-PtCl$_2$-NH-C$_{10}$H$_7$]$^+$, 407.1 [PtCl$_2$-NH-C$_{10}$H$_7$]$^+$, 281.2 [PtCl$_2$-NH-]$^+$, 267.3 [PtCl$_2$]$^+$
[Pt(*pa*)$_2$Cl$_2$] (**2**)	456.2	454.7 [M]$^+$, 418.8 [PtCl(*pa*)$_2$]$^+$, 384.1 [Pt(*pa*)$_2$]$^+$, 359.9 [PtCl$_2$(*pa*)]$^+$, 298.8 [-HN-PtCl$_2$-NH-]$^+$, 283.3 [PtCl$_2$-NH-]$^+$, 97.1 [*pa*]$^+$
[Pt(*aph*)$_2$Cl$_2$] (**3**)	636.4	638.9 [MH]$^+$, 563.9 [Pt(*aph*)$_2$]$^+$, 417.1 [PtCl(*aph*)]$^+$, 381 [Pt(*aph*)]$^+$, 299.1 [-HN-PtCl$_2$-NH-]$^+$, 184.2 [*aph*]$^+$, 92.1 [C$_6$H$_5$-NH-]$^+$

In the mass spectra the appearance of molecular ions and different fragments demonstrate the formation of the complexes, and they are in agreement with the decomposition results of thermal analysis.

^{1}H and ^{13}C NMR measurements

^{1}H- and ^{13}C-NMR measurements were carried out for the complexes in DMSO-d_6. The characteristic chemical shifts for the prepared complexes are listed below.

[Pt(*an*)$_2$Cl$_2$], ^{1}H-NMR: The amine groups protons appear at 7.96 – 7.78 ppm and the aromatic rings protons are between 7.14 – 7.92 ppm.

[Pt(*pa*)$_2$Cl$_2$], ^{1}H-NMR: The amine groups protons appear at 6.62 – 6.69 ppm and the aromatic rings protons are between 8.04 – 8.68 ppm. They are shifted to higher values due to the presence of N atoms in the aromatic ring. ^{13}C-NMR: The aromatic ring signals are between 158.4 – 161.2 ppm for the carbons, which are near to the nitrogen atoms and the others are at 110.63 – 111.16 ppm.

[Pt(*aph*)$_2$Cl$_2$], ^{1}H-NMR: The amine groups protons appear at 6.57 ppm and the aromatic rings protons are between 6.7 – 7.41 ppm. The HO group proton is at 10.4 ppm.

FT-IR spectra

The broad bands in the spectrum of all three compounds (Fig. 1) at about 3200 cm^{-1} can be assigned to overlapped NH and CH stretching of the amino groups and aromatic rings. The somewhat lower intensity of νNH of the secondary amine in the spectrum of **3** is in accordance with lower number of N–H bonds compared to the primary amine analogues (**1** and **2**), having several overlapped peaks in the region 3400 − 3000 cm^{-1}. The other difference is a low intensity peak in the spectrum of **3** at 3732 cm^{-1} (Fig. S1) due to the stretching of its hydroxyl substituent of the phenyl ring. The most intensive bands in the spectra of all three samples appear in the region ~1600 – 1450 cm^{-1} due to the C=C stretching of the aromatic rings. Below 1500 cm^{-1} NH bending of coordinated amines is combined with νC=C. Owing to its nitrogen-containing heterocycle, the complex **2** has several strong, sharp peaks in this IR region with a νC=N band at 1562 cm^{-1}. Peaks of C–N vibrations appear in all spectra at ~1350 – 1200 cm^{-1}, and peaks of νC–C are present at about 1100 cm^{-1}. One of the most important peaks supporting the formation of complexes is the νPt–N at 518 – 692 cm^{-1}. The νPt–Cl peaks appear between 445 – 496 cm^{-1}. The position of these peaks is influenced by the nitrogen atoms in the aromatic ring. For νPt–N and νPt–Cl, the lowest wavenumbers were found in the case of [Pt(*pa*)$_2$Cl$_2$], which means that these bonds are stronger compared to those in the other complexes.

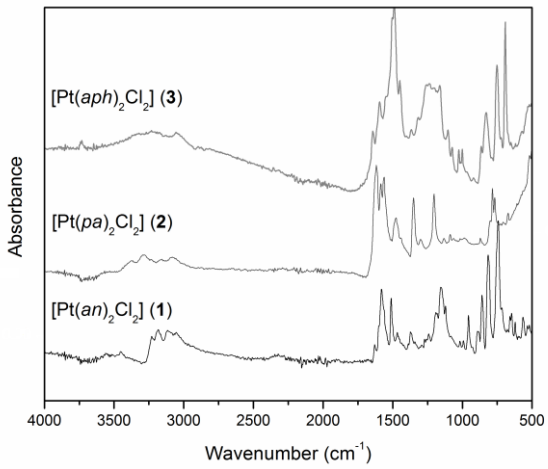

Fig. 1 FT-IR spectra of the complexes

Thermal properties

The thermal measurements were carried out in nitrogen and air. All three complexes contain adsorbed water, which evaporates in inert N_2 atmosphere starting already at room temperature (Fig. 2). Although the elemental analysis data for complex $[Pt(an)_2Cl_2]\cdot 2H_2O$ (**1·2H$_2$O**) suggest two molecules of lattice water (6.13 %), the mass loss for water evaporation up to ~160 °C is significantly lower (1.2 %). It is explained by spontaneous evaporation of water between the time of elemental analysis and thermal measurements. In $[Pt(aph)_2Cl_2]$ (**3**) the water evaporation slows down above 100 °C, but it is not completely finished until the decomposition of the compound begins at ~130 °C. The absorbed water content (~1.7 %) in complex $[Pt(pa)_2Cl_2]$ (**2**) completely evaporates to 100 °C and the anhydrous compound is stable up to ~175 °C. The anhydrous complex **2** is the most stable one in the series. The thermal stability of complexes decreases in the order **2** > **1** > **3**. The thermal degradation of all three complexes is continuous without stable intermediate formation. The mechanism of decomposition is different depending upon composition and structure. After water release, on the DTG curve of **1** three peaks with maxima at 194, 294 and 343 °C can be observed. In these decomposition steps **1** looses most of its aminonaphtalene ligands and coordinated chlorides. Differently, **3** has only one DTG peak and it looses the fragments of ligands in only one decomposition step at 223 °C. The lowest stability of **3** can be explained by its bulky ligands and steric effects (Scheme 1). Above 400 °C the decomposition for both **1** and **3** slows down but does not end up to 700 °C. The several overlapping processes of **2** with DTG peaks at 323, 545 and 593 °C suggest a more complex decomposition mechanism, compared to that of the other two compounds, which is in accordance with the structural differences between complexes. Namely, **2** is the only complex with a heterocyclic ligand, while in **1** and **3** ligands with aromatic hydrocarbon rings are coordinated. The mass loss (21.7 %) of **2** suggests that the evaporation of fragments of heterocyclic ligand starts along with the loss of coordinated chlorides (15.98 %) at 300 °C. The thermal decomposition of **2** is not also finished in nitrogen until 700 °C.

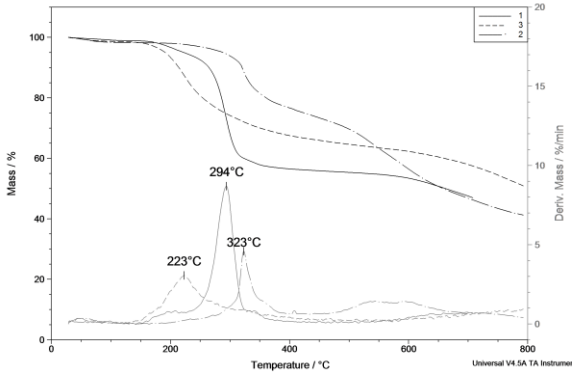

Fig. 2 TG and DTG curves of **1** (——), **2** (- - -) and **3** (– · –) in N_2

The DTA curves of the compounds (Fig. 3) show that below 100 °C there is an endothermic peak on all three curves due to the absorbed water evaporation. Then their thermal decomposition in inert atmosphere is followed by an exothermic thermal effect. The most intensive decomposition steps of complexes **1** and **2** are also endothermic with peak maxima at 296 and 326 °C. Furthermore, on the DTA curve of **2** a small exothermic peak is observed at 204 °C without significant mass change at this temperature. The thermal decomposition of compound $[Pt(aph)_2Cl_2]$ (**3**) is followed by an exothermic effect with a small peak at 217 °C due to its oxygen content.

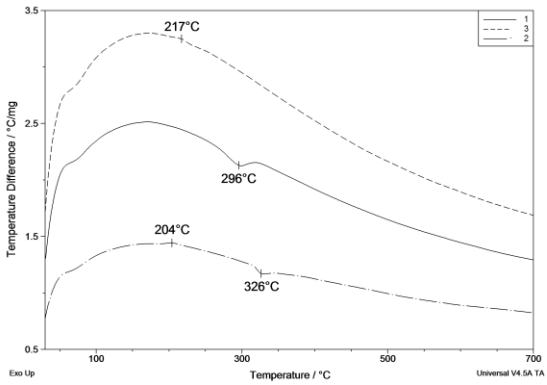

Fig. 3 DTA curves of compounds **1** (⟶), **2** (- - -) and **3** (– · –)

The thermal properties of the samples in air are somewhat different from those in nitrogen. The decomposition mechanism of **2** in air is also different from the other two complexes. Its first decomposition DTG peak is less intensive and appears at somewhat higher temperature than in nitrogen (Fig. 4). The overlapped peaks of the next decomposition steps at 425, 455 and 477 °C in air are more intensive and shifted to lower temperatures, compared with DTG peak maxima in nitrogen at 545 and 593 °C.

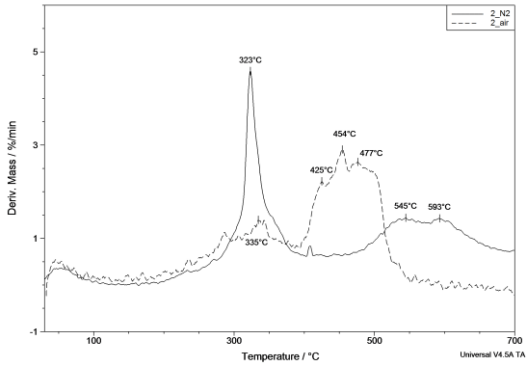

Fig. 4 DTG curves of $[Pt(pa)_2Cl_2]$ (**2**) in N_2 (⟶) and air (- - -)

The mechanism of thermal degradation of **1** does not depend on the nature of atmosphere up to ~250 °C. Above this value a highly exothermic decomposition process starts followed by the melting of the sample. Complex **3** in air also decomposes in an intensive exothermic process, starting with the melting of the sample. In oxidative atmosphere (air) samples **1** and **3** get burned, resulting in deformed exothermic peaks on the DTA curves.

TG-MS data

TG/DTG curves do not allow the proper identification of the fragments of compounds; thus, on-line coupled TG/DTG-MS measurements were carried out for all three complexes (Fig. 5).

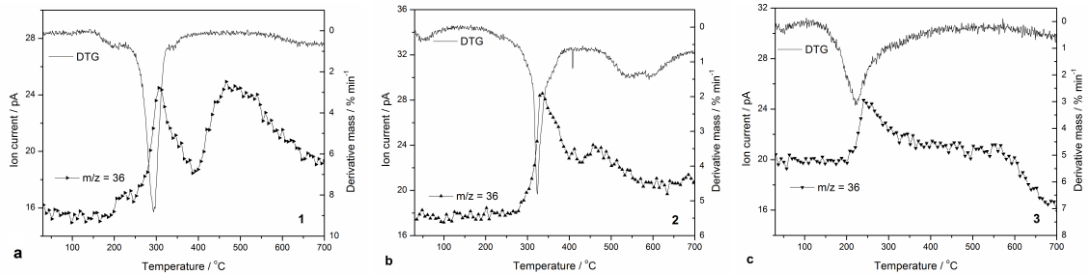

Fig. 5 MS peaks of m/z = 36 for **1** (a), **2** (b) and **3** (c)

Beside the thermal techniques the water content of complexes was proved by signals for *m/z* = 18 and 17. Their relative intensity is in accordance with the evaporation of the absorbed water for all three compounds. Corresponding to the general formula ($PtCl_2R_2$) of samples, evaporation of HCl (*m/z* = 36) is also detected in all samples during the most intensive decomposition step at 294, 323 and 223 °C for **1**, **2** and **3**, respectively. The peaks for *m/z* = 36 at temperatures above 400 °C, without mass change, most probably belong to fragments of organic ligands e.g. $C_5H_{12}^{2+}$ or $C_4NH_{10}^{2+}$. Howeve, most fragments depart at lower temperatures in all cases, as the amount of formed fragments above 400 °C is low and their evaporation is practically undetectable by TG/DTS without coupled mass spectrometer. The other fragments reflect the composition of the complexes. In compounds **1** and **3** bearing ligands with aromatic rings, the detected peaks are characteristic for benzene ($C_6H_6^+$) with *m/z* = 78 and 77 and for acetonitrile ($C_2H_3N^+$) with *m/z* = 41. Acetonitrile fragment is forming during the decomposition of the aromatic rings. These fragments are not detected in **2** because its heterocyclic ligand gives different fragments. Beside benzene, during the thermal decomposition of **1**, naphthalene ($C_{10}H_8^+$) with *m/z* = 128 and recombined fragments [38] with low *m/z* values of 41, 43 ($C_2NH_5^+$), 50 ($C_4H_2^+$) and 55 ($C_4H_7^+$) (Scheme 2a) are detected (Fig. S2). Since complex **3** also has amine ligand with aryl substituents (Scheme 1), beside the same fragments as in **1** (Scheme 2b), peaks are observed for *m/z* = 91, characteristic for phenol and *m/z* 66 for $C_4H_2O^+$ [38] (Fig. S3). On the basis of composition and structure of **3**, the splitting of OH group would be expected with a peak at *m/z* 17. However, its absence suggests that this sample does not loose fragments OH^+ or NH_3^+ with molar mass of 17. Since *m/z* 16 and 15 can be characteristic for amine group also, the lack of the peaks for these *m/z* values shows that the amine group of the ligand evaporates as part of some larger fragments (Scheme 2b). It can be resulted by increasing the NH – Ar (Ar = aromatic ring) bonds stability after loosing one aryl substituent. It is supposed that these changes affect the ring aromaticity and the stability of bonds within it, and lead to formation of fragments with lower molar mass, e.g. $C_2H_3N^+$ (*m/z* = 41) and $C_4H_2O^+$ (*m/z* = 66). The detected fragments of complex **2** with relatively low molar mass (Fig. S4) show that during its thermal decomposition the bonds in 2-pyrimidinamine ligands break up and recombine giving molecular ions with low molar masses, as $CN_2H_3^+$ with *m/z* = 42, $C_2NH_5^+$ with *m/z* = 43 or C_3NH^+ with *m/z* = 51 (Scheme 2c). A characteristic peak for the heterocyclic ring is not detected. It proves the lower stability of pyrimidine ring due to its N heteroatoms, compared to benzene.

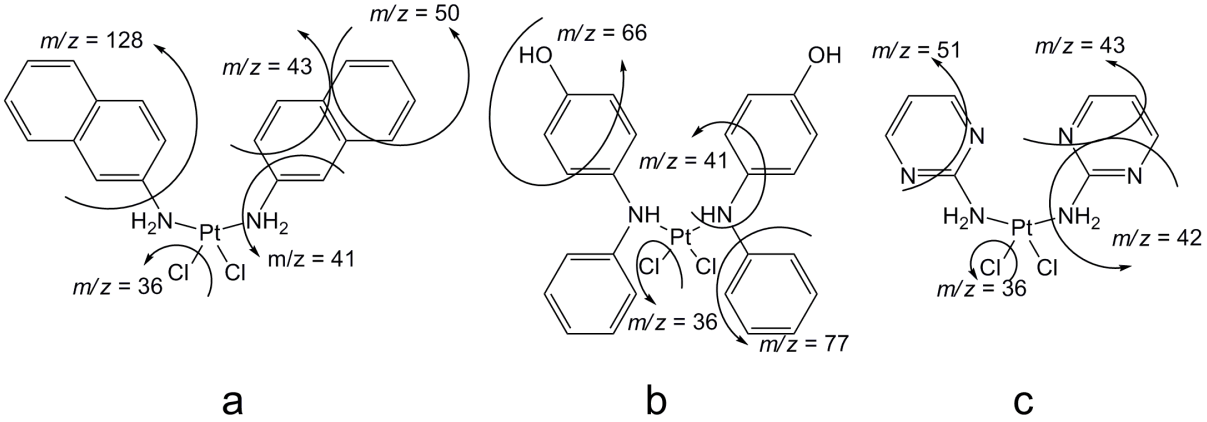

Scheme 2 Characteristic fragments of compounds **1** (a), **3**(b) and **2**(c)

Antimicrobial tests

All three compounds show antimicrobial activity. Their bacteriostatic effect on the microorganisms is represented with diameters of inhibition zones of bacteria spreading . Generally, they are more effective inhibitors of Gram(+) than Gram(−) bacteria (Table 3). The newly synthesized **3** is the most active sample with the wider zones of inhibition. **1** shows similar bacteriostatic activity against *S. aureus*, *S. ventriculi* and somewhat lower against *E. coli*. Its inhibition zones in the case of *B. subtilis* and *K. oxytoca* are significantly less. Complex **2** is the least active sample and it is inactive toward *E. coli*. These differences in bacteriostatic effect can be explained by their different structures and composition of the complexes and agree well with their different thermal stability.

Namely, compound **3** of the lowest stability is the most effective against tested bacteria. In general terms, complexes with more lipophilic ligands in their structure are found to have higher antibacterial activity. Probably, the lipophilic character of the complexes can result in increased damage of bacterial cell wall and also facilitate their transport through bacterial cell membranes, so they can reach their cellular targets more efficiently [39,40].

Our results show that compound **3** exhibits the lowest stability and proved to be the most effective inhibitor of the microbial development, interfering mainly with the growth of Gram(+) bacteria. The lower inhibitory effect on the growth of Gram(−) bacteria could be related with the complexity of the cell wall of these microorganisms.

A possible reason for the highest activity of **3** is the reactive OH substituent of 4-anilinophenol (*aph*) ligands. To prove this hypothesis, the bacteriostatic activity of the analogue compound with diphenylamine (*dpa*) ligand [Pt(*dpa*)$_2$Cl$_2$] was also tested. It is only active toward *S. aureus* and *S. ventriculi* with 7 and 13 mm bacteriostatic zone diameters, respectively. The significantly lower activity of [Pt(*dpa*)$_2$Cl$_2$] compared to **3** confirms that OH group plays an important role in inhibition of bacterial growth.

The Pt-complexes tested seem to have a moderate antimicrobial potential and further investigations are required to enhance their inhibitory effect.

Table 3 The diameters of bacteriostatic zones of the complexes (mm)

	Gram(+) bacteria			Gram(−) bacteria	
Complexes	*Staphylococcus aureus*	*Bacillus subtilis*	*Sarcina ventriculi*	*Klebsiella oxytoca*	*Escherichia coli*
[Pt(*an*)$_2$Cl$_2$] (**1**)	15	13	23	9	13
[Pt(*pa*)$_2$Cl$_2$] (**2**)	9	13	9	9	inactive
[Pt(*aph*)$_2$Cl$_2$] (**3**)	17	21	23	13	17

Conclusions

A new Pt(II) complex with 4-anilinophenol (*aph*) ligand was synthesized (**3**), while new preparation route was developed for **1** and **2**. The *aph* ligand, similar to the 2-aminonaphtalene and 2-pyrimidinamine ligands in the complexes **1** and **2**, is coordinated in a monodentate mode through its amino nitrogen atom. The other two coordination sites are occupied by chlorine atoms. The complexes precipitate in mostly amorphous form. All compounds contain absorbed water which starts to evaporate at room temperature. Among the anhydrous complexes, **2** is the most stable one in the inert atmosphere, and the complex stability is decreasing in the order **2** > **1** > **3**. The thermal decomposition in all cases is continuous without stable intermediate formation. The thermal degradation of **1** and **3** in air is followed by the burning of the samples and therefore their thermal curves are deformed. By on-line coupled TG/DTA-MS measurements, beside the evaporation of water and HCl, the

fragments characteristic for the aromatic rings of the ligands were detected. All compounds show bacteriostatic effect. Their antimicrobial activity is decreasing in the order: **3** > **1** > **2**, and it is in agreement with their thermal stability. The new compound **3** with the lowest stability shows the highest bacteriostatic effect.

Acknowledgements

The authors wish to express their thankfulness to the "Domus Hungarica Foundation" of Hungary for the several fellowships provided to Berta Barta Holló and Csaba Várhelyi jr.
I. M. Szilágyi thanks for a János Bolyai Research Fellowship of the Hungarian Academy of Sciences. An OTKA-PD-109129 grant is acknowledged.

References

[1] Wheate NJ, Walker S, Craig GE, Oun R. The status of platinum anticancer drugs in the clinic and in clinical trials. Dalton Trans. 2010;39:8113–8127.

[2] Wani WA, Prashar S, Shreaz S, Gómez-Ruiz S. Nanostructured materials functionalized with metal complexes: In search of alternatives for administering anticancer metallodrugs. Coord Chem Rev. 2016;312:67–98.

[3] Wang Z, Wua M, Gou S. Toward a better understanding of the oxaliplatinmode of action upon the steric hindrance of 1,2-diaminocyclohexane and its analogue. J Inorg Biochem. 2016;157:1–7.

[4] Benedetti M, De Castro F, Romano A, Migoni D, Piccinni B, Verri T, Lelli M, Roveri N, Fanizzi FP. Adsorption of the *cis*-$[Pt(NH_3)_2(P_2O_7)]^{2-}$ (*phosphaplatin*) on hydroxyapatite nanocrystals as a smart way to selectively release activated *cis*-$[Pt(NH_3)_2Cl_2]$ (*cisplatin*) in tumor tissues. J Inorg Biochem. 2016;157:73–79.

[5] Mavroidi B, Sagnou M, Stamatakis K, Paravatou-Petsotas M, Pelecanou M, Methenitis C. Palladium(II) and platinum(II) complexes of derivatives of 2-(4'-aminophenyl)benzothiazole as potential anticancer agents. Inorg Chim Acta. 2016;444:63–75.

[6] Kelland L. The resurgence of platinum-based cancer chemotherapy. Nat Rev Cancer. 2007;7:573–584.

[7] Chen J, Li K, Swavey S, Church KM. Synthesis, characterization and DNA binding activity of $PtCl_2$[DMSO][N4[N-3(4-pyridylmethyl)thymidine]]. Inorg Chim Acta. 2016;444:76–80.

[8] Gaber M, El-Ghamry HA, Fathalla SK. Ni(II), Pd(II) and Pt(II) complexes of (1*H*-1,2,4-triazole-3-ylimino)methyl]naphthalene-2-ol. Structural, spectroscopic, biological, cytotoxicity, antioxidant and DNA binding. Spectrochim Acta A. 2015;139:396–404.

[9] Timerbaev AR, Hartinger CG, Aleksenko SS, Keppler BK. Interactions of Antitumor Metallodrugs with Serum Proteins: Advances in Characterization Using Modern Analytical Methodology. Chem Rev. 2006;106:2224–2248.

[10] Zanvettor NT, Nakahata DH, de Paiva REF, Ribeiro MA, Cuin A, Corbi PP, Formiga ALB. Copper(II), palladium(II) and platinum(II) complexes with 2,2-thiophen-yl-imidazole: Synthesis, spectroscopic characterization, X-ray crystallographic studies and interactions with calf-thymus DNA. Inorg Chim Acta. 2016;443:304–315.

[11] Saenger W, Orth P, Kisker C, Hillen W, Hinrichs W. The Tetracycline Repressor-A Paradigm for a Biological Switch. Angew Chem Int Ed. 2000;39:2042–2052.

[12] Speer BS, Shoemaker NB, Salyers AA. Bacterial Resistance to Tetracycline: Mechanisms, Transfer, and Clinical Significance. Clin Microbiol Rev. 1992;5:387–399.

[13] Guerra W, Silva IR, Azevedo EA, de S. Monteiro AR, Bucciarelli-Rodriguez M, Chartone-Souza E, Silveira JN, Fontes APS, Pereira-Maia EC. Three new complexes of platinum(II) with doxycycline, oxytetracycline and chlortetracycline and their antimicrobial activity. J Braz Chem Soc. 2006;17:1627–1633.

[14] Shiju C, Arish D, Bhuvanesh N, Kumaresan S. Synthesis, characterization, and biological evaluation of Schiff
base–platinum(II) complexes. Spectrochim Acta A. 2015;145:213–222.

[15] Rahman FU, Ali A, Khan I, Guo R, Chen L, Wang H, Li ZT, Lin Y, Zhang DW. Synthesis and characterization of trans-Pt(II)(salicylaldimine)(pyridine/pyridine-4-carbinol)Cl complexes: In vivo inhibition of E. coli growth and in vitro anticancer activities. Polyhedron. 2015;100:264–270.

[16] Mansour AM, Abdel-Ghani NT. Synthesis, spectroscopic, DFT, cytotoxicity and antimicrobial activity of Pd(II) and Pt(II) complexes of N,N-chelated benzimidazole derivatives. Inorg Chimi Acta. 2015;438:76–84.

[17] Abdel-Ghani NT, Mansour AM. Palladium(II) and platinum(II) complexes containing benzimidazole ligands: Molecular structures, vibrational frequencies and cytotoxicity. J Mol Struct. 2011;991:108–126.

[18] Sabounchei SJ, Shahriary P, Salehzadeh S, Gholiee Y, Chehregani A. Spectroscopic, theoretical, and antibacterial approach in the characterization of 5-methyl-5-(3-pyridyl)-2,4-imidazolidenedione ligand and of its platinum and palladium complexes. C. R. Chimie. 2015;18:564–572.

[19] Sabounchei SJ, Shahriary P, Salehzadeh S, Gholiee Y, Nematollahi D, Chehregani A, Amani A, Afsartala Z. Pd(II) and Pd(IV) complexes with 5-methyl-5-(4-pyridyl)hydantoin: Synthesis, physicochemical, theoretical, and pharmacological investigation. Spectrochim Acta A. 2015;135:1019–1031.

[20] Szilágyi IM, Deák A, Várhelyi Cs jr., Madarász J, Pokol G, Gömöry Á, Várhelyi Cs. Structural and thermal study of assymetric α-dioxime complexes of Co(III) with Cl and methyl-pyridines. Polyhedron. 2010;10:2185–2189.

[21] Mansour AM. Thermal, spectral, DFT and biological activity evaluation of Co(II), Ni(II) and Cu(II) complexes of N,S-chelated benzotriazole ligand. J Therm Anal Calorim. 2016;123:571–581.

[22] Soliman MH, Hindy AMM, Mohamed GG. Thermal decomposition and biological activity studies of some transition metal complexes derived from mixed ligands sparfloxacin and glycine. J Therm Anal Calorim. 2014;115:987–1001.

[23] Zayed EM, Zayed MA, Hindy AMM. Thermal and spectroscopic investigation of novel Schiff base, its metal complexes, and their biological activities. J Therm Anal Calorim. 2014;116:391–400.

[24] Arora S, Aneja DK, Kumar M, Sharma C, Prakash O. Thermal studies of some biological active oxadiazoles. J Therm Anal Calorim. 2013;111:17–25.

[25] Fernandes LP, Oliveira WP, Sztatisz J, Szilágyi IM, Novák Cs. Solid state studies on molecular inclusions of lippia sidoides essential oil obtained by spray drying. J Therm Anal Calorim. 2009;95:855–863.

[26] Giron D. Investigations of polymorphism and pseudo-polymorphism in pharmaceuticals by combined thermoanalytical techniques. J Therm Anal Calorim. 2001;64:37–60.

[27] Schmidt C, Senfter N, Griesser UJ. Crystal polymorphism of local anaesthetic drugs. J Therm Anal Calorim. 2003;73:397–408.

[28] Noordin MI, Chung LY. Thermostability and polymorphism of theobroma oil and palm kernel oil as suppository bases. J Therm Anal Calorim. 2009;95:891–894.
[29] Thorey P, Bombicz P, Szilágyi IM, Molnar P, Bansaghi G, Szekely E, Simandi B, Parkanyi L, Pokol G, Madarasz J. A novel no-crystal of (R,R)-1,2-cyclohexanediol with (R,R)-tartaric acid, a key structure for resolution of the racemic (±)-trans-diol in supercritical carbon dioxide, and the binary melting phase relations. Thermochim Acta. 2010;497: 129–136.
[30] Holló B, Magyari J, Živković-Radovanović V, Vučković G, Tomić ZD, Szilágyi IM, Pokol G, Mészáros Szécsényi K. Synthesis, characterization and antimicrobial activity of bis(phthalazine-1-hydrazone)-2,6-diacetylpyridine and its complexes with CoIII, NiII, CuII and ZnII. Polyhedron. 2014;80:142–150.
[31] Giron D, Goldbronn C. Place of DSC purity analysis in pharmaceutical development. J Therm Anal Calorim. 1995;47:217–251.
[32] Todeschini V, de Oliveira PR, Bernardi LS, Pereira RL, de Campos CEM, Silva MAS, Volpato NM. Delapril and manidipine characterization and purity evaluation in raw materials, J Therm Anal Calorim. 2014;115:2295–2301.
[33] Várhelyi Jr. Cs, Kuzmann E, Homonnay Z, Lengyel A, Pokol Gy, Izvekov V, Szalay R, Kun A, Tomoaia-Cotişel M, Covaci E, Garg VK, Oliveira AC, Goga F. Preparation and characterization of novel
[Fe(methylisopropylglyoximato)$_2$(amine)$_2$] mixed chelates. J Radioanal Nucl Chem. 2015;304:745–750.
[34] Gabano E, Gama S, Mendes F, Gariboldi MB, Monti E, Bombard S, Bianco S, Ravera M. Study of the synthesis, antiproliferative properties, and interaction with DNA and polynucleotides of cisplatin-like Pt(II) complexes containing carcinogenic polyaromatic amines. J Biol Inorg Chem. 2013;18:791–801.
[35] Mishra LK. Complexes of palladium(II) and platinum(II) with some organic ligands. J Ind Chem Soc. 1982;59:408–409.
[36] Beveridge TJ. Use of the gram stain in microbiology. Biotech Histochem. 2001;76:111–118.
[37] Stewart EJ, Madden R, Paul G, Taddei F. PLoS Biol. 2005;3:295–300.
[38] NIST Webbook. http://webbook.nist.gov/chemistry. Last time accessed 26 September 2015.
[39] Chang EL, Simmers C, Knight DA. Cobalt Complexes as Antiviral and Antibacterial Agents. Pharmaceuticals. 2010;3:1711–1728.
[40] Utku S, Topal M, Döğen A, Serin MS. Synthesis, characterization, antibacterial and antifungal evaluation of some new platinum(II) complexes of 2-phenylbenzimidazole ligands. Turk J Chem. 2010;34:427–436.